NOLTR 66-42

A STUDY OF THE ROLE OF MECHANICAL-STRENGTH PROPERTIES ON THE PHENOMENA OF SPALLATION

4 JANUARY 1966

NOL

UNITED STATES NAVAL ORDNANCE LABORATORY, WHITE OAK, MARYLAND

UNCLASSIFIED
NOLTR 66-42

Ballistics Research Report 157

A STUDY OF THE ROLE OF MECHANICAL-STRENGTH PROPERTIES ON THE PHENOMENA OF SPALLATION

Prepared by:
Robert Piacesi and James W. Watt

ABSTRACT: An experimental investigation was made to determine the role of mechanical-strength properties on the spallation phenomena due to hypervelocity impact. The size of the impacting particle and the thickness of the target (1.5 inches) were held constant, while the impacting velocity and the yield strength of the target were varied. The target materials were 7075-T6 Al and 7075-0 Al. The magnitude of the shock pressure arriving at the back surface of the target was monitored by observing the motion of aluminum dust particles pushed off the back surface by the shock wave. The spall thickness and amount of deformation of the spalled piece were measured. It was shown that the yield strength influences the amount of deformation for two reasons: it controls the strength of the shock that is propagated through the materials, as well as determines the resistance of the material to begin to plastically deform. The amount of deformation could be calculated with good agreement with experiment using the theory of Hopkins and Prager for the deformation of thin, plastic, circular plates by an impulse load.

U. S. NAVAL ORDNANCE LABORATORY
WHITE OAK, MARYLAND

NOLTR 66-42 4 January 1966

A STUDY OF THE ROLE OF MECHANICAL-STRENGTH PROPERTIES ON THE PHENOMENA OF SPALLATION

This report is part of an experimental program to investigate the basic phenomena associated with the impact of hypervelocity particles onto various targets.

J. A. DARE
Captain, USN
Commander

a. E. Seigel
A. E. SEIGEL
By direction

CONTENTS

ILLUSTRATIONS

LIST OF SYMBOLS

C_0	elastic-wave speed in aluminum, 16,700 fps
I	impulse
m	mass
P	pressure
P_0	yield strength
ℓ	thickness of spall
U	shock-wave velocity
u	particle velocity
V_0	impact velocity
V_c	crater volume
V_p	projectile volume
w	deformation
ρ_o	density of undisturbed medium
τ	time associated with impulse loading
μ	mass per unit cross-sectional area

INTRODUCTION

When a high-speed projectile impacts a semi-infinite plate, a shock wave is transmitted into both the projectile and the plate. An extremely large stress is developed by the passage of the shock wave, so large that the deviatoric component of the stress may be ignored, and the process may be treated in a hydrodynamic manner. Indeed, this type of analysis is used for solving the initial phase of the impact process by computer hydrodynamic flow codes, references (1), (2) and (3). This high pressure causes the projectile and plate material to flow and to be ejected backward from the plate at high velocities at the initial part of the process (see figure 1). As a result of this flow process, a crater is formed similar to that shown in figure 2.

Figure 3 illustrates the nature of the stress-waves propagated into the plate. This figure shows the impact of a 1/4-inch aluminum sphere on a 2-inch-thick lucite plate at a velocity of 19,400 feet per second. A spherically diverging shock wave with its origin at the point of impact is propagated through the medium. As this wave interacts with the free surface of the plate at the impact side, a shear wave is produced which also propagates into the target medium. In a semi-infinite medium, this spherical shock is attenuated and is reduced first to an elastic-plastic wave and eventually to an elastic wave.

In the case of a plate of finite thickness, as in figure 3, this compressive wave is reflected from the free surface of the back side of the plate as a tension wave. That part of the spherical wave which reaches the free surface other than normal to it, produces upon reflection both a dilatational tension wave and a shear wave. At a point where the magnitude of the tension produced by this reflected wave exceeds the dynamic-fracture strength of the material, a fracture will occur. This process is known as spallation, references (4) and (5). Figure 4 shows the type of fracture produced by hypervelocity impact.

As stated earlier, at a time near the instant of impact the stress is high and may be considered as a pressure and the material may be considered as a fluid. Hence, the hydrodynamic or Hugoniot properties of the material are important during the initial phase of the crater formation. This stress is quickly dissipated and reduced to a level where the elastic-plastic properties of the medium are important. The size of the crater produced then should depend on both the hydrodynamic and the elastic-plastic properties of the medium.

It was previously shown by Piacesi, Waser and Dawson, reference (6), that the yield strength of the medium, an elastic-plastic property, was the important mechanical-strength property in determining the crater size due to hypervelocity impact. The experiment consisted of impacting several aluminum alloys, having a range of mechanical strengths, with 1/4-inch-diameter aluminum spheres at high velocities. The yield strength of the highest strength target was measured as a function of temperature. It was shown that when this high-strength target was heated to an appropriate temperature such that its yield strength was reduced to that of a lower strength target, which was kept at room temperature, equal size craters were obtained when these two targets were impacted by spheres at the same velocity.

The object of the work discussed in this report was to investigate the characteristics of spallation resulting from hypervelocity impact as a function of the mechanical-strength properties of the target medium. In particular, such spall characteristics as the attenuation of the shock strength, the spall-fracture location, and amount of bulging of the rear surface were investigated as a function of the target-yield strength. In this study, the yield strength of the higher strength target was again varied by heating the target as was done in the above-mentioned experiments on cratering.

O'Brien, reference (7), has shown that the spall strength for aluminum is approximately 13 kbars, which agrees well with our measurements (see figure 9A), and is independent of impurity content, degree of working, or temperature. In our work, only one alloy was used (7075 Al in the annealed and T6 condition); therefore, the investigation then was reduced to being dependent only on the nature of the stress-waves propagated in the heated and unheated targets and their yield strength, and not on the spall strength. Although the value of the peak stress arriving at the rear surface was measured in our work, the wave shape was not measured because of the difficulty in doing so.

EXPERIMENTAL PROCEDURE

A description of the hypervelocity impact facility is given in Appendix A. (See figure 11.)

Aluminum spheres, 1/4 inch in diameter, were used as the projectiles. The spheres were accelerated to velocities up to 22,000 feet per second by a two-stage light-gas launcher. The targets were circular plates of an aluminum alloy, 8 inches in diameter and 1.5 inches thick. A calrod heater

element was coiled around the side of the target for heating. The temperature of the heated targets was monitored by imbedding an iron-constantan thermocouple into a hole drilled into the side of the target.

The target materials used were 7075-0 aluminum and 7075-T6 aluminum with room temperature yield strengths of 18,800 psi and 62,500 psi, respectively. Figure 5 shows the yield strength of the 7075-T6 Al as a function of temperature. It is seen that at 500°F the 7075-T6 Al has a yield strength equivalent to the 7075-0 at room temperature.

The peak pressure of the shock wave at the time which it reflects from the rear surface is determined by measuring the material-particle velocity behind the shock and using the Hugoniot equation of state for aluminum, references (8), (9) and (10).

The relationship between the shock velocity and particle velocity for 24 ST Al, reference (10), which is assumed to be valid for the alloy used in this experiment, is

$$U \frac{cm}{\mu sec} = .535 + 1.34\, u \qquad (1)$$

where U is the shock velocity, and u is the particle velocity. The pressure is determined from the relationship

$$P = \rho_0 U u \qquad (2)$$

where ρ_0 is the density of the undisturbed material.

The particle velocity behind the shock, u, is determined by observing the motion of aluminum dust particles which have been pushed off the back surface by the interaction of the shock wave with the rear surface. The experiments were conducted in a vacuum in order to eliminate the air drag on the dust particles. The backs of the targets are sanded to insure that an adequate number of particles are pushed off to observe their motion more clearly. A Beckman-Whitley 192 high-speed camera was used to record their displacement with time. A 1/2-inch square grid is placed at the target position and exposed on the film prior to conducting the impact experiment. This provides a scale to relate the particle motion to an absolute velocity. Figure 1 shows several frames of pictures from the 80-frame series for a single-impact firing. The

camera can be made to record on 35-mm film up to rates of approximately 750,000 frames per second. The film is then "read" on a telereader. This optical-electronic instrument projects the picture onto a large screen (magnification is approximately 25X) where the x,y coordinates can be read out electronically after adjusting a set of cross hairs at the desired point. Figure 6 shows a typical particle displacement-time plot from which the velocity can be determined. The actual particle velocity behind the shock, however, is one-half the velocity of the particles emanating from the back surface due to the reflection of the wave as a tension wave, reference (10). This technique which is a modification of the pellet "throw-off" technique, references (4) and (12), has several advantages over the pellet technique. One advantage is that the dust does not need to be aligned carefully to the point of impact as does the pellet since the dust covers the entire back surface of the target. Also it more truly represents the particle velocity behind the reflected shock front.

RESULTS

Figure 7 is a log-log plot of the normalized-crater volume, Vc/Vp, vs the normalized-impact velocity, Vo/Co, where Vc is the crater volume, Vp is the original projectile volume, Vo is the impact velocity and Co is the elastic-wave speed in room-temperature aluminum. The crater volume created in the finite-thickness plate was larger for a given velocity than the crater created in a semi-infinite target. As in the previous experiments, however, the yield strength for the finite plate proved to be the correlation parameter as far as crater volume was concerned.

The spall location depends on the wave shape, as well as the critical-fracture stress for the material. In this experiment, no attempt was made to determine the wave shape. It was not possible then to predict the position of the fracture. However, the value of the peak stress arriving at the target rear surface was determined for many of the impacts by the particle velocity technique as discussed previously.

It was expected that the fracture position would change with the impact velocity because the wave shape would change over the range of velocities covered in this work. The fracture position, however, was approximately 3.5 mm from the rear surface in all cases. The fractures were quite jagged so that the exact location was obscured, making it difficult

to pinpoint any small differences in their location. Small differences would be expected since the general shape of the wave would be approximately a steep triangle.

The amount of bulging that the rear surface, i.e., the spalled piece, undergoes depends upon two things: the magnitude of the stress wave reaching the back surface (which depends on the yield strength of the material as will be discussed later), and the yield strength of the material. This can be seen when one combines the information given in figures 8, 9, and 10.

Figure 8 shows the amount of bulging of the rear surface as a function of the impact velocity. The 7075-0 Al, having a yield strength of 18,800 psi, was impacted over a range of velocities, and the data were seen to be joined by a smooth curve. The 7075-T6 Al was impacted at temperatures of 200°F, 300°F, and 500°F, having yield strengths of 56,000 psi, 44,000 psi, and 18,700 psi, respectively, and compared with the curve for the 7075-0 Al. The deformations were slightly higher for the 7075-0 Al over the entire velocity range covered for the case where the yield strengths of both materials were equal (7075-0 at 72°F, 7075-T6 at 500°F). However, as shown in figure 9A, this result is consistent with the fact that the pressure magnitude of the shock wave arriving at the rear surface for the same impact velocity was slightly higher for the 7075-0 Al. For clarification, note that this pressure does not actually exist on the rear surface itself since the boundary conditions require that it be zero. It is probable that the heated target attenuates the wave somewhat more than the unheated for equal yield strengths, but not enough to significantly influence the spallation and deformation for the target thicknesses used in these tests.

At an impact velocity of 26,000 feet per second into the 7075-T6 Al at 200°F the peak pressure of the shock wave arriving at the rear surface is equivalent to that of the 7075-0 Al impacted at only 18,900 psi. Although the peak pressures are equal, the deformations that the spalled pieces suffer are quite different. The 7075-0 Al having the lower yield strength underwent a much greater deformation. This demonstrates that the yield strength does influence the amount of deformation.

It should be noted also in figure 8 that, at about 19,000 feet per second, the deformation increases rapidly for the 7075-0 and the 500°F 7075-T6 materials. This can be understood from figure 9A which is a plot of the peak pressure arriving at the rear surface vs impact velocity. It is

seen that the peak pressure also increases rapidly at an impact velocity of approximately 19,000 feet per second.

Figure 9B is a plot of the pressure at impact vs the peak pressure at the rear surface for the 7075-0 Al. The pressure at impact is calculated from the one-dimensional impact theory and the Hugoniot equation of state for aluminum which was used previously. This plot shows, in somewhat an artificial manner, the attenuation of the peak pressure for a target thickness of 1.5 inches.

The amount of deformation that occurs can be calculated quantitatively to a surprising degree of agreement with experiment as seen in figure 10. The theory used here is that of Hopkins and Prager which predicts the deformation of simply supported thin plates by an impulse loading. Appendix B describes the manner in which the impulse of the shock was calculated and employed in the theory.

CONCLUSIONS

The location of the spall fracture was not sensitive over the range of impact velocities covered in this experiment. The amount of bulging of the spalled section, however, was extremely sensitive with impact velocity and could be directly correlated with the peak stress of the shock wave which arrives at the rear surface and with the yield strength of the material. Furthermore, the peak stress arriving at the rear surface for a given impact velocity was seen to be dependent on the yield strength. In conclusion, it was shown that the yield strength governs the amount of deformation of the rear surface spall for two reasons: it influences the strength of the shock that is propagated through the material, as well as determines the resistance of the material to begin to plastically deform. The amount of deformation could be calculated with good agreement with experiment using the theory of Hopkins and Prager for the deformation of thin, plastic, circular plates by an impulse load.

REFERENCES

(1) Bjork, R. L., "Numerical Solutions of the Axially Symmetric Hypervelocity Impact Process Involving Iron," Proceedings of Third Symposium on Hypervelocity Impact, Vol I, Feb 1959

(2) Walsh, J. M. and Tillotson, J. H., Proceedings of the Sixth Symposium on Hypervelocity Impact, Vol II, Part I, 1959

(3) Heyda, J. F. and Riney, T. D., "Penetration of Structure by Hypervelocity Projectiles," Space Science Laboratory, General Electric Company

(4) Rinehart, J. S., "Some Quantitative Data Bearing on the Scabbing of Metals under Explosive Attack," Journal of Applied Physics, Vol 22, No. 5, pp 555-560, May 1951

(5) Rinehart, J. S., "Scabbing of Metals under Explosive Attack: Multiple Scabbing," Journal of Applied Physics, Vol 23, No. 11, pp 1229-1233, Nov 1952

(6) Piacesi, R., Waser, R. H., and Dawson, V. C. D., "Determination of the Yield Strength as an Important Mechanical Strength Property in Hypervelocity Impact," Seventh Hypervelocity Impact Symposium, Tampa, Florida, Nov 1964

(7) O'Brien, J. L., "The Fracture of Metals Under Impulsive Loading Conditions," Harvard University, Division of Engineering and Applied Physics, Doc. 35-61-12, Dec 1961

(8) Walsh, J. M., et al, "Shock Wave Compressions of Twenty-Seven Metals," Phys. Rev. 108, pp 196-216, 1957

(9) Al'Tshuler, L. V., et al, Soviet Physics, JETP, 11, 573, 1960

(10) Rice, M. H., et al, "Solid State Physics," Vol 6, pp 61-62, Academic Press, Inc., N. Y., 1958, Editors F. Seitz and D. Turnbull

(11) Piacesi, R. and Waser, R. H., "Multiple Piston Two-Stage Light Gas Launcher," NOLTR 64-96, Aug 1964

(12) Kinslow, R., "Properties of Spherical Stress Waves Produced by Hypervelocity Impact," AEDC-TDR 63-197, Oct 1963

(13) Hopkins, H. G. and Prager, W., "On the Dynamics of Plastic Circular Plates," Z. angew. Math. Phys., 5, 317-330, 1954

APPENDIX A

DESCRIPTION OF HYPERVELOCITY IMPACT FACILITY

The test facility used for this program was the U. S. Naval Ordnance Laboratory Hypervelocity Impact Range No. 1. This range is a 30-foot long, 6-foot diameter tube, which can be evacuated to less than 1 mm Hg pressure and which is equipped with projectile velocity measuring instrumentation consisting of light screens and time interval counters. A Beckman-Whitley 192 high-speed framing camera and a high intensity flash tube light source having a 100 sec duration was used to photograph the impact of the projectile with the test targets. A 0.500-inch two-stage light gas gun was used to accelerate the 0.250-inch aluminum sphere projectiles to velocities up to 22,000 feet per second, reference (11). Figure 11 is a photograph of the facility and figure 12 is a schematic of the facility. The X-ray sources are associated with the velocity measuring system to provide a positive check on its operation by photographing the projectile that triggers the light screens. The projectiles were mounted in bore size lexan sabots which were stripped off and deflected as they left the muzzle.

APPENDIX B

CALCULATION OF THE DEFORMATION OF THE REAR SURFACE

Hopkins and Prager, reference (13), theoretically obtained the following relationship for the permanent deflection of the center of a simply supported thin plastic circular plate due to a uniformly applied dynamic loading

$$\omega = \frac{I^2 \left(1.5 - \frac{P}{P_0}\right)}{2 \mu P_0} \qquad (1)$$

where w is the deflection, I is the square wave impulse, Po is the yield strength of the plate material, P is the stress magnitude of the square wave, and μ is the mass per unit cross-sectional area.

The spalled material was then treated as a thin circular plate being dynamically loaded by the stress which caused the spallation and the above theory was used to calculate the deformation.

The spall strength was taken to be 13 kbar or 188,500 psi (see figure 8A and reference (7)) and the wave shape was assumed to be approximately triangular. The average stress applied then to the spalled piece is obtained from the relation

$$P = \frac{2x \text{ (peak pressure at back surface)} - 188{,}500}{2} \qquad (2)$$

The time that this pulse acts is the time it takes for the pulse front to traverse the thickness of the spall in both directions. The velocity of the pulse U is obtained from the relation

$$U \ \frac{cm}{\mu SEC} = .535 + 1.34\, U \qquad (3)$$

where U is the material particle velocity immediately behind the wave front. The period, τ, then is

$$\tau = \frac{2 \times \ell}{U} \tag{4}$$

where ℓ is the thickness of the spall, which was taken to be 3.5 mm for the calculation of the theoretical curve in figure 10. The impulse then is

$$I = P\tau$$

The mass per unit cross-sectional area, μ, is

$$\mu = \rho_o \ell \tag{5}$$

where ρ_o is the density of the material.

This calculation assumes that the impulse at the center of the spalled piece is applied uniformly over the entire piece. This means that the shear wave, which is produced by the parts of the compression wave that arrive at the back surface other than normal, is not taken into account and that the peak stress measured at the rear surface is the average peak stress acting on the spalled piece.

A certain minimum deformation should occur if the material fractures since a finite amount of momentum is "trapped" by the spalled piece. This was calculated by assuming a triangular pulse having a peak stress exactly equal to the assumed spall strength of 13 kbars. The spall thickness was chosen to be 3.5 mm. This minimum value for the deformation is represented as the lower terminating point of the theoretical line in figure 10.

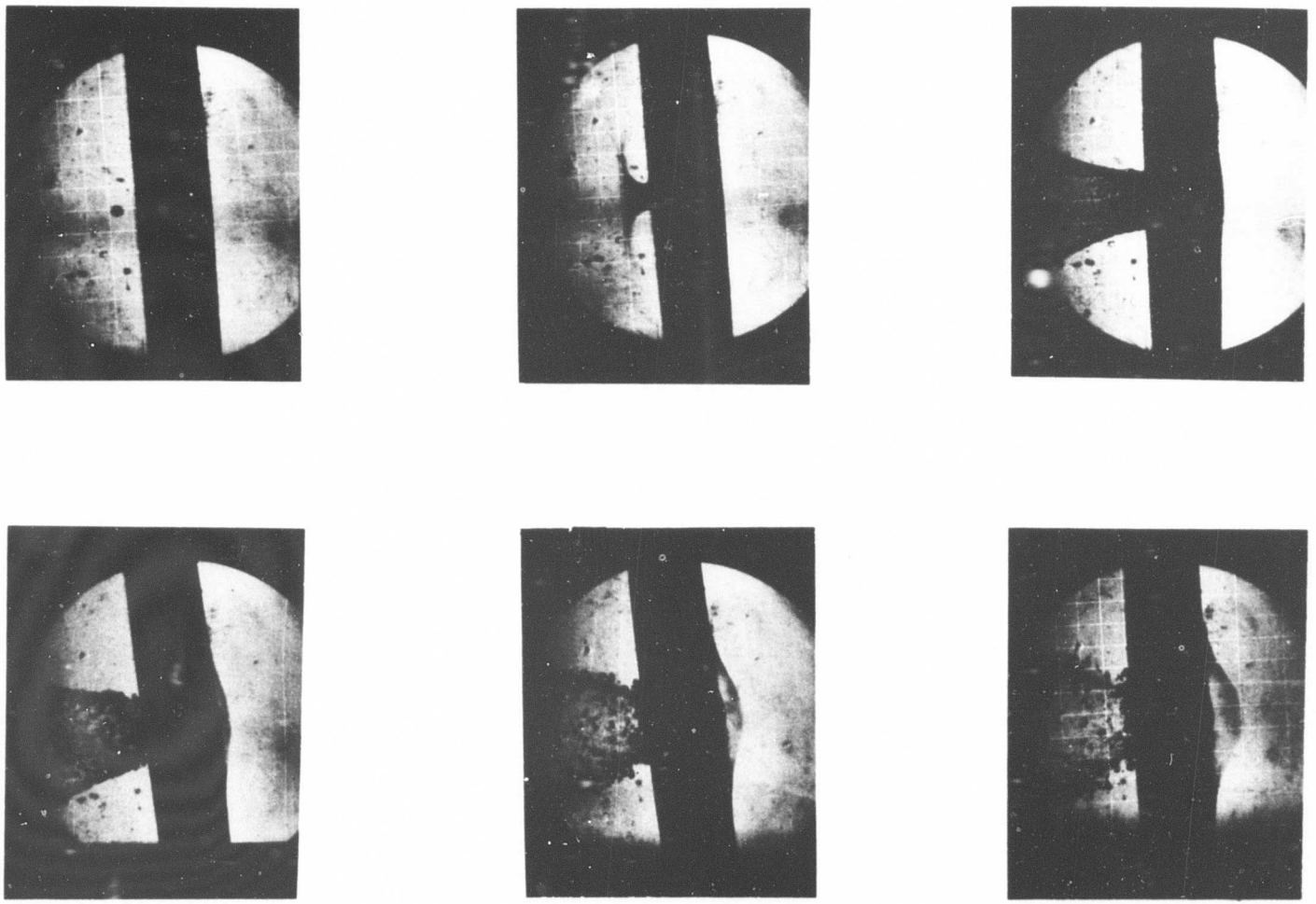

FIG. 1 IMPACT OF ALUMINUM SPHERE ONTO ALUMINUM PLATE

FIG. 2 CRATER FORMED IN ALUMINUM TARGET BY IMPACT OF 1/4 INCH ALUMINUM SPHERE AT VELOCITY OF 18,000 FPS

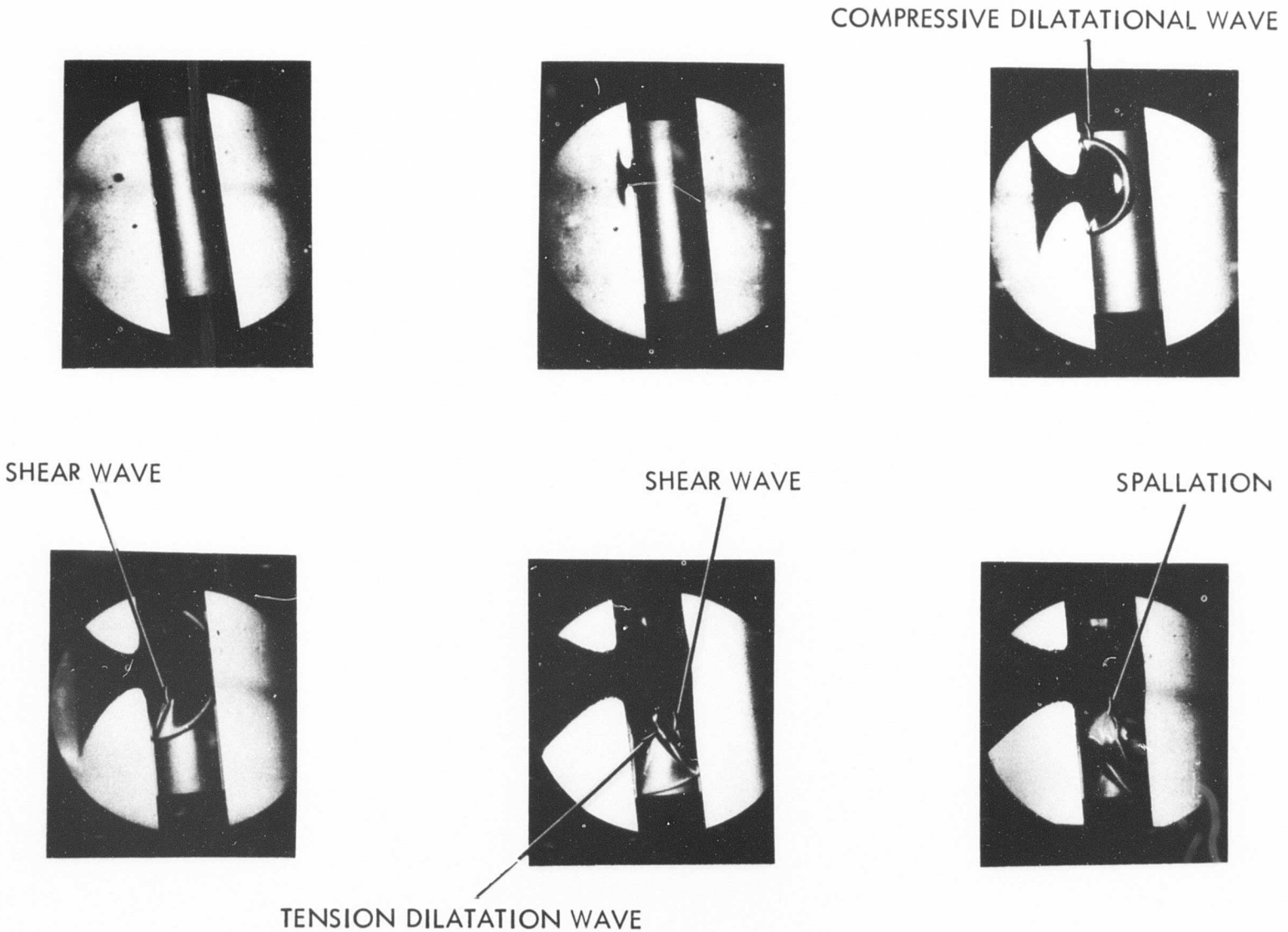

FIG. 3 IMPACT OF ALUMINUM SPHERE ONTO LUCITE PLATE

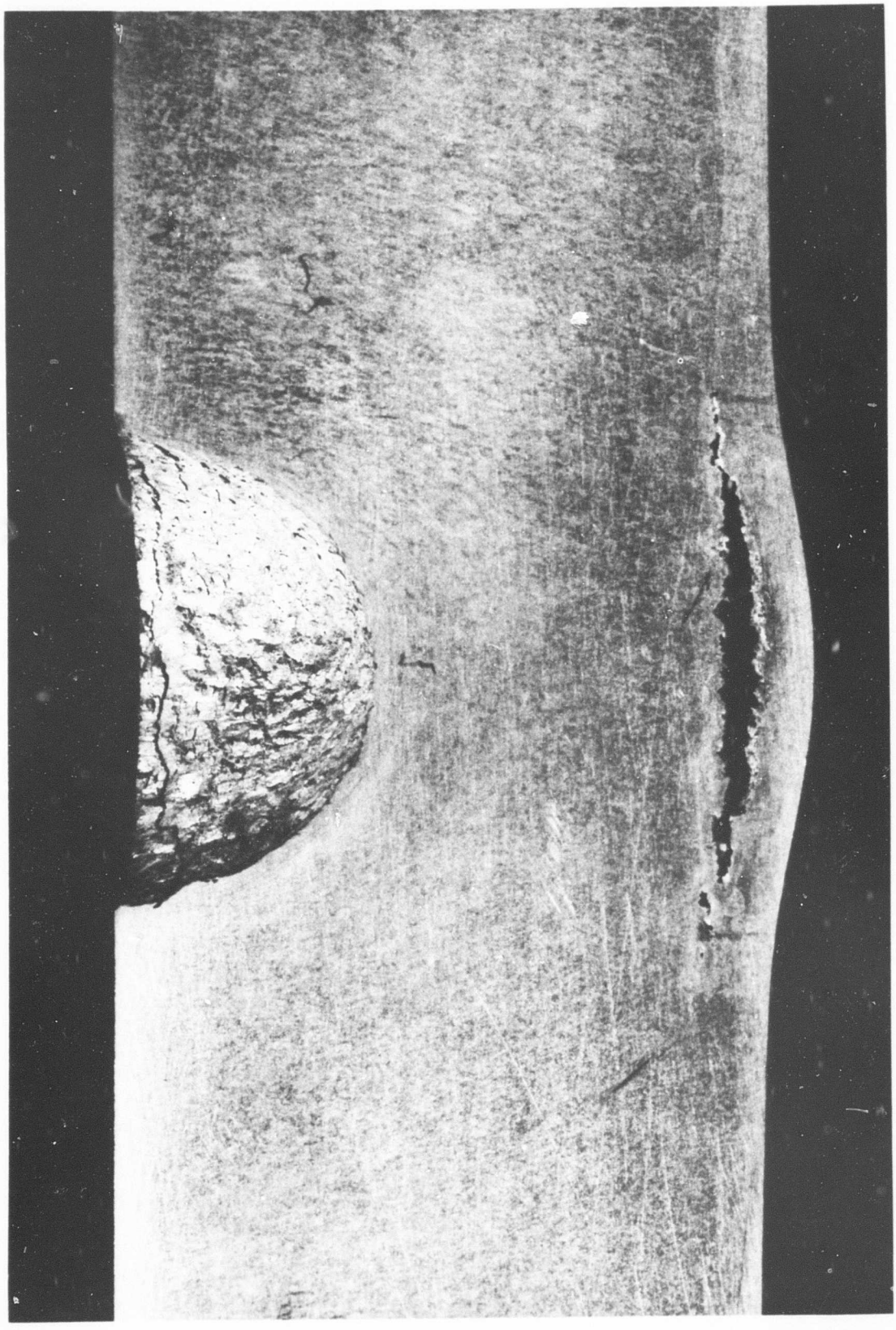

FIG. 4 ALUMINUM TARGET WITH SPALLATION

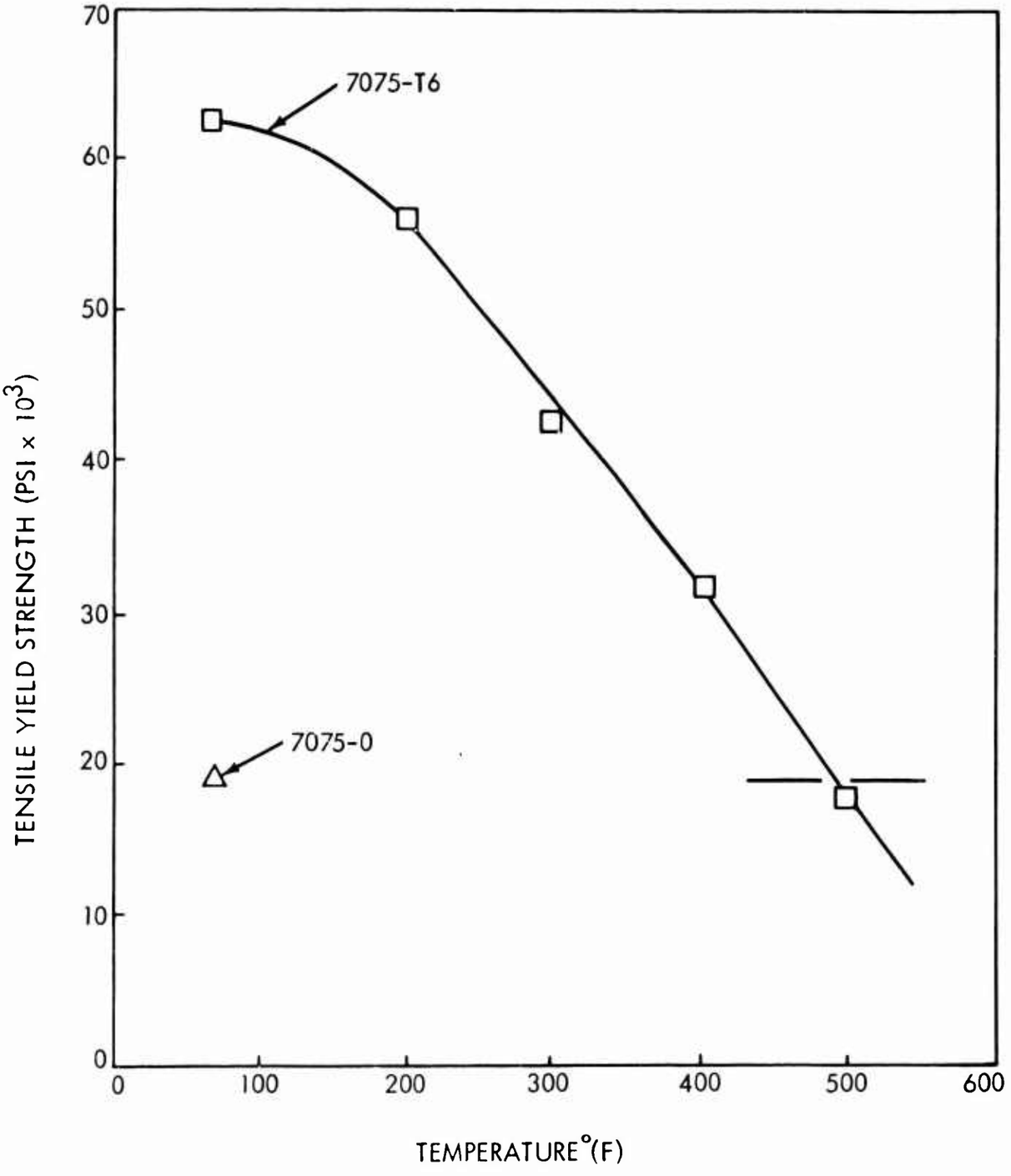

FIG. 5 TENSILE YIELD STRENGTH VS TEMPERATURE

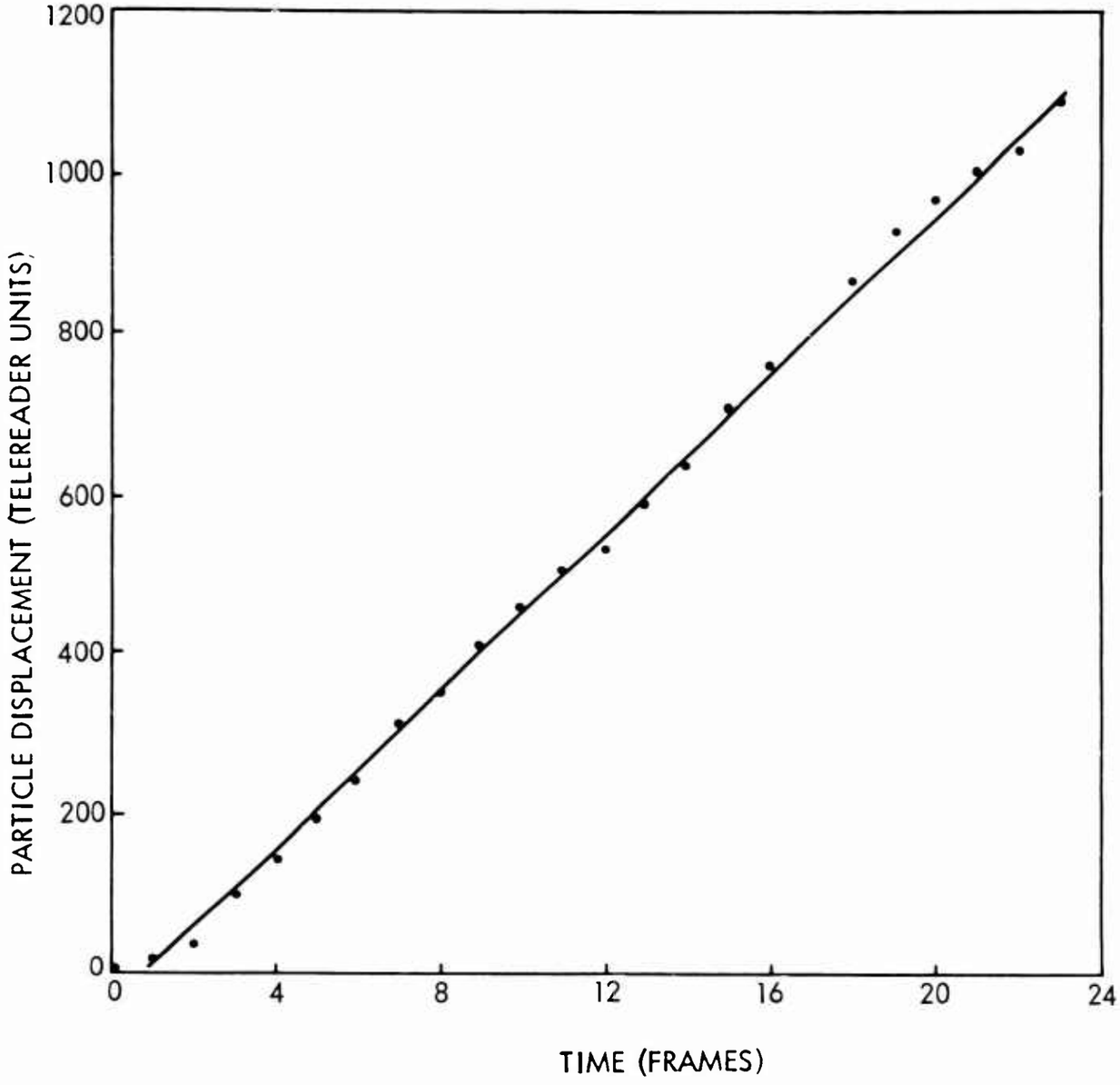

FIG. 6 MOTION OF PARTICLES PUSHED OFF THE REAR OF THE TARGET BY THE SHOCK WAVE

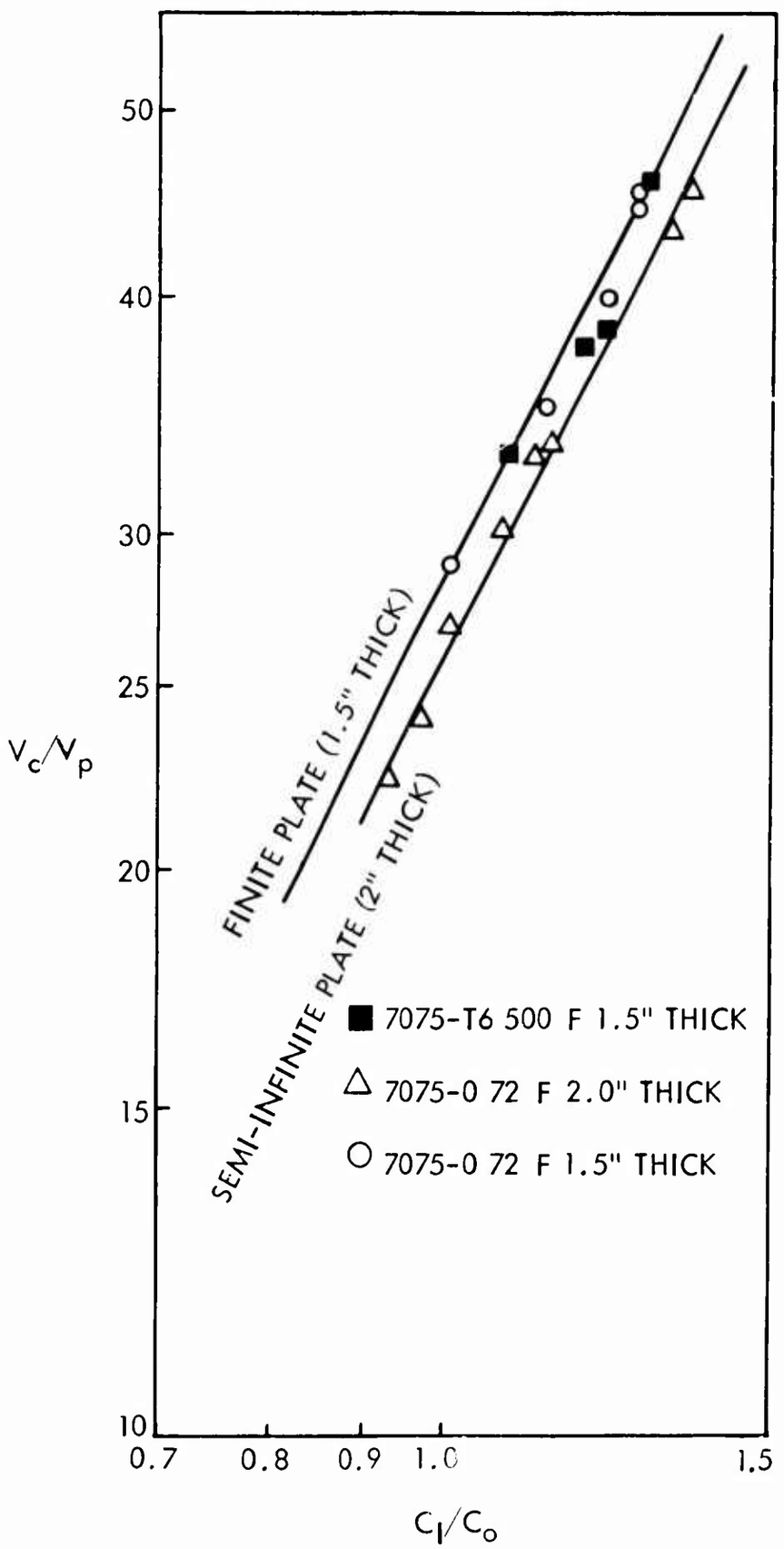

FIG. 7 CRATER VOLUME VS IMPACT VELOCITY

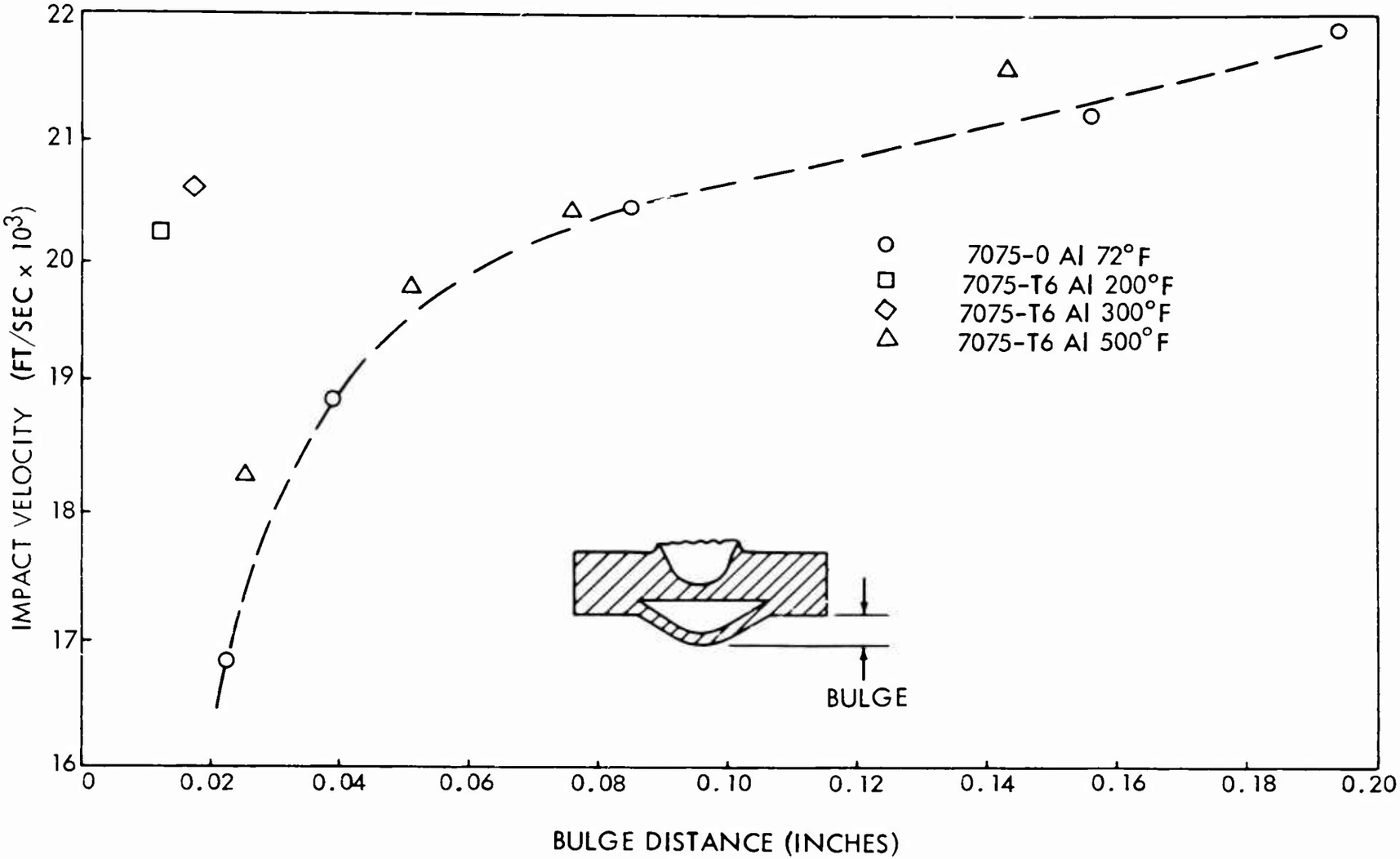

NOLTR 66-42

FIG. 8 DEFORMATION OF REAR SURFACE

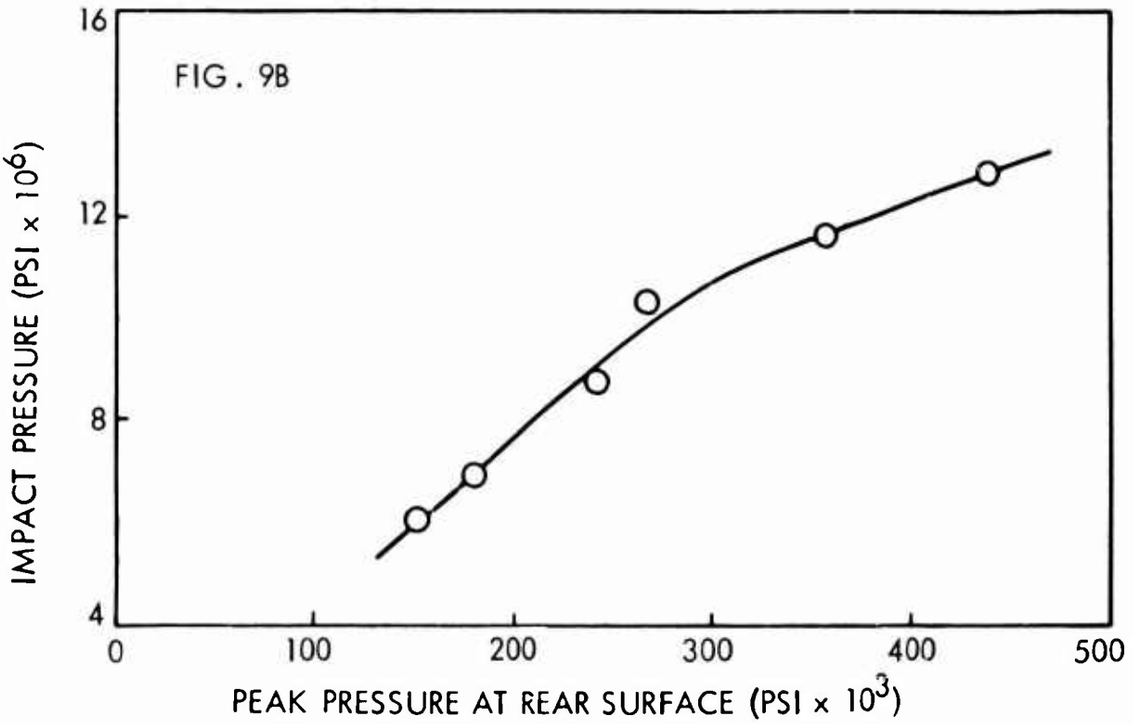

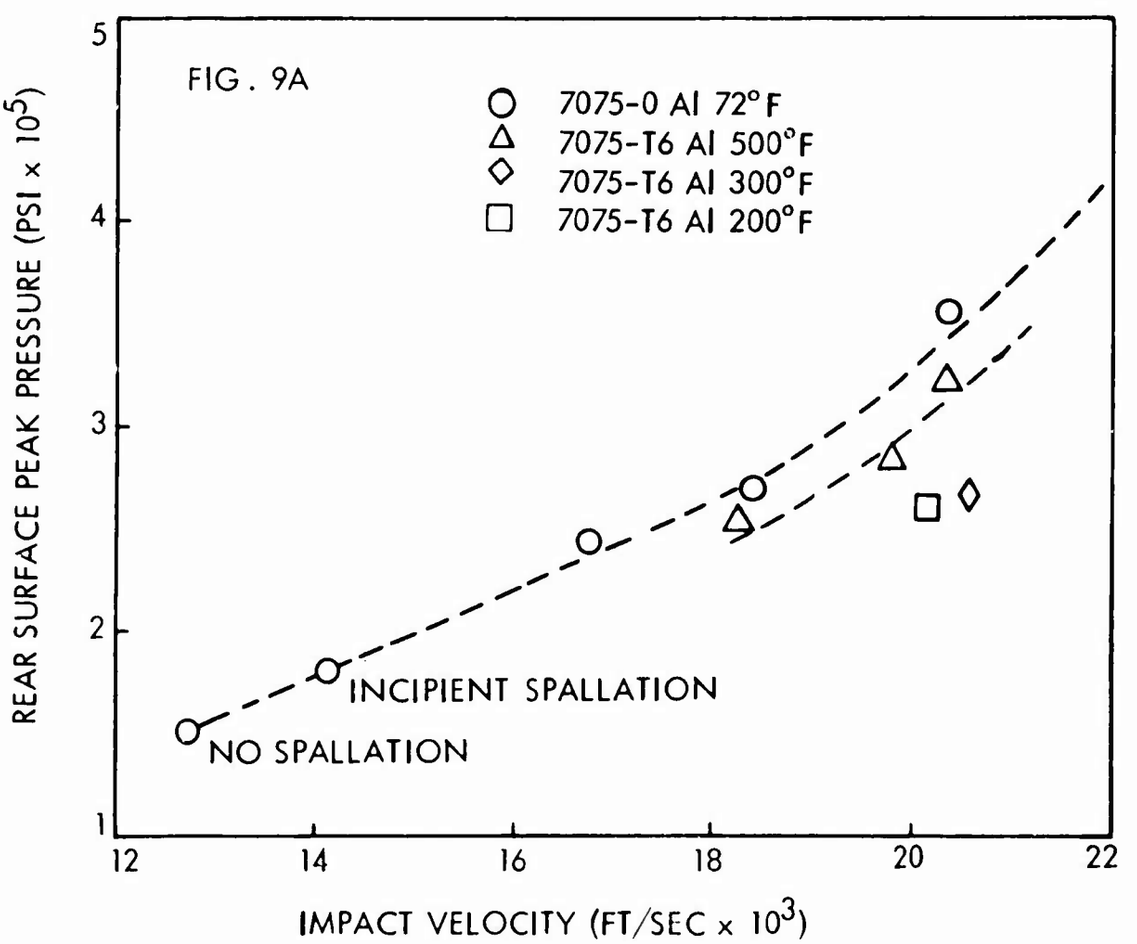

FIG. 9 PRESSURE RELATIONS

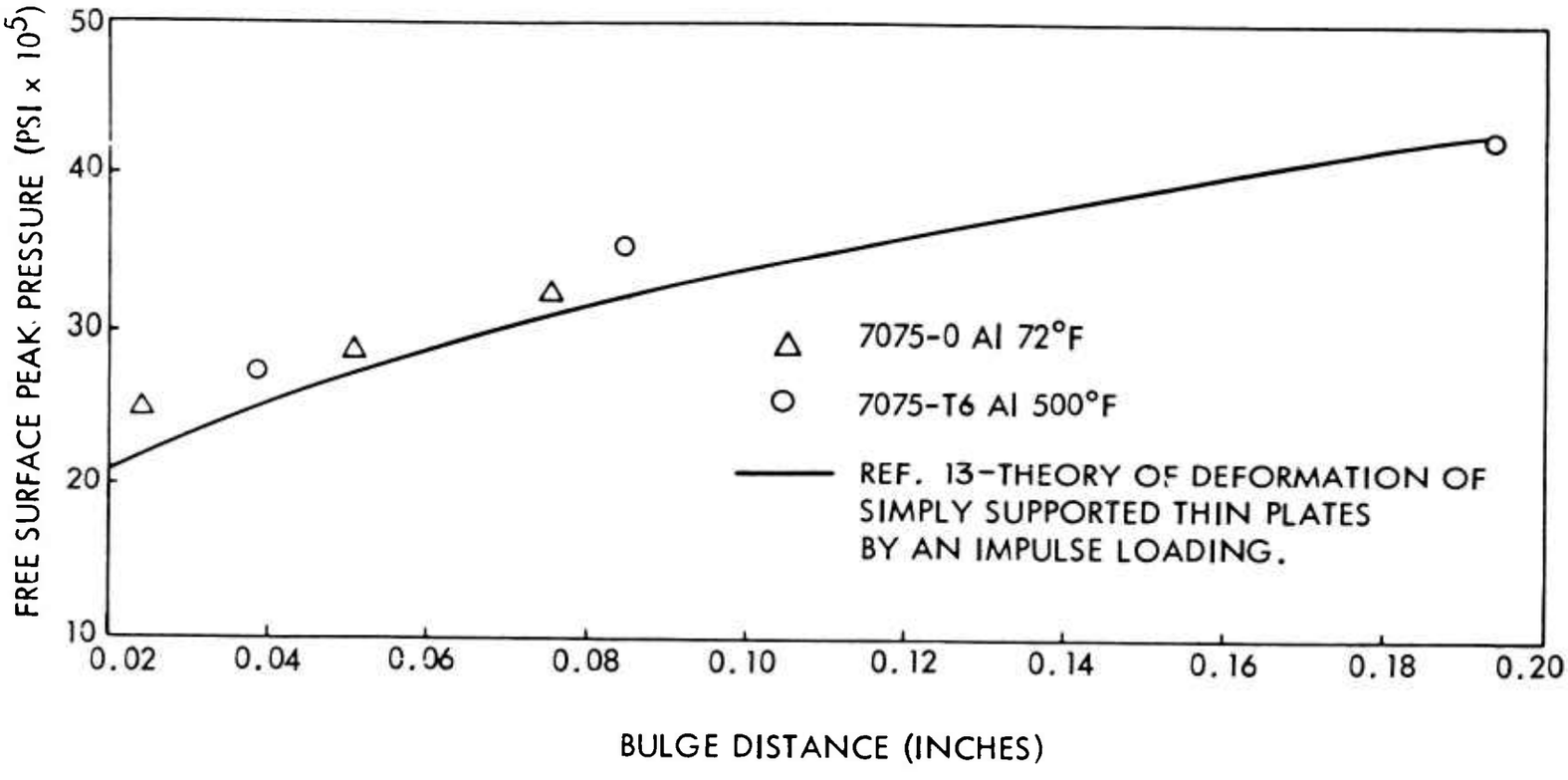

FIG. 10 DEFORMATION OF THIN PLATES BY IMPULSIVE LOADING

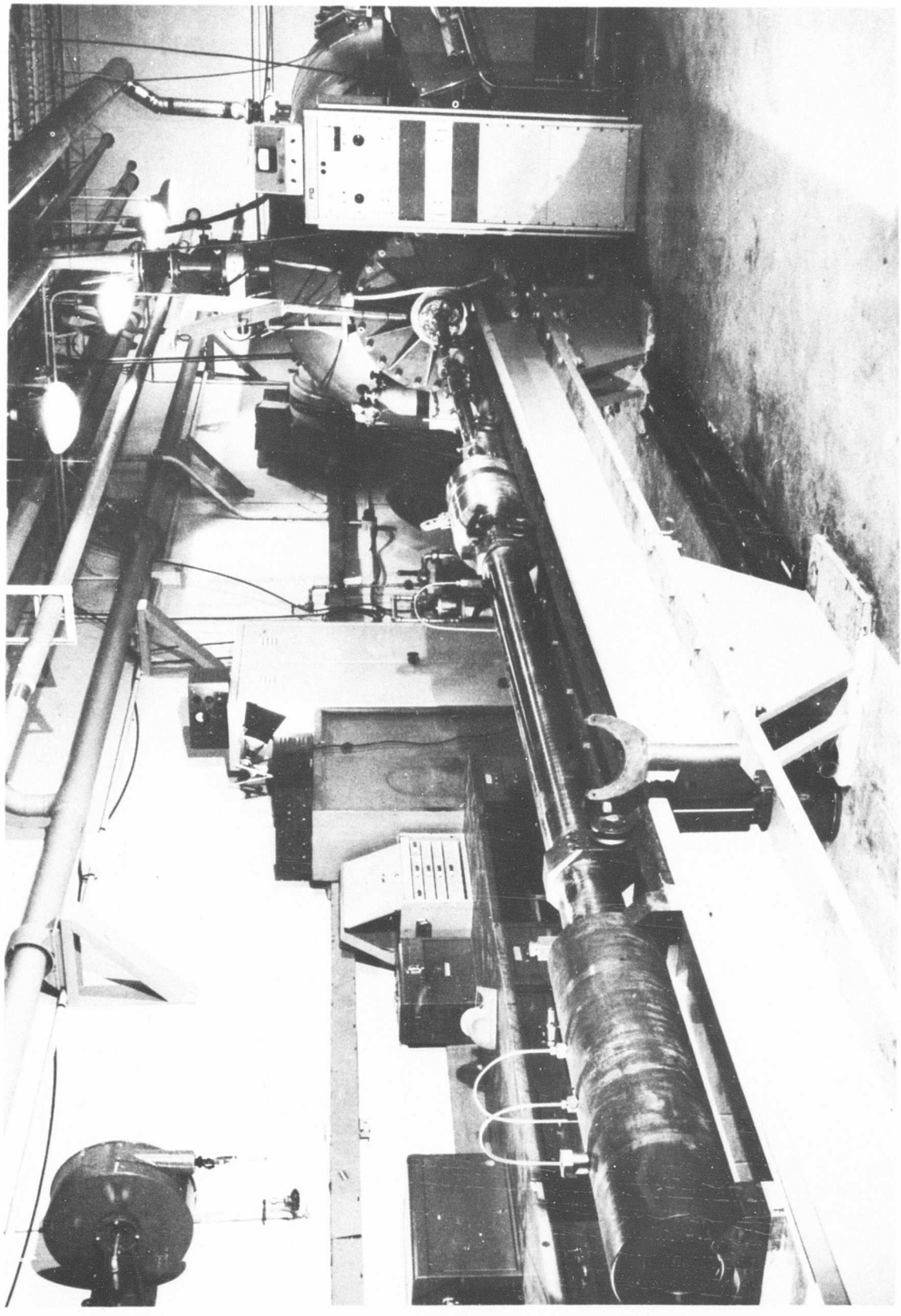

FIG. 11 NOL HYPERVELOCITY IMPACT FACILITY

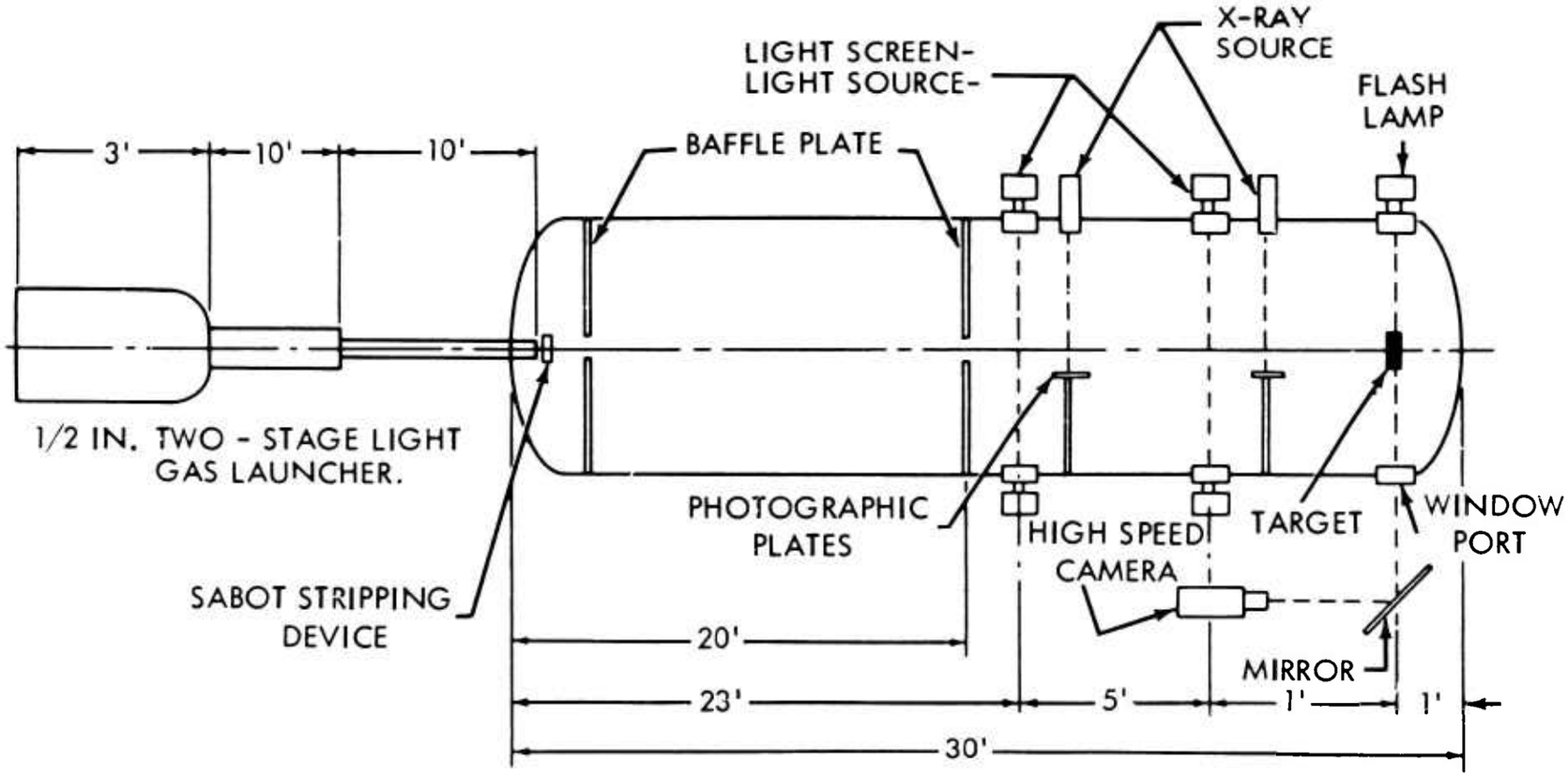

FIG. 12 SCHEMATIC OF N.O.L. HYPERVELOCITY IMPACT RANGE

UNCLASSIFIED

Security Classification

DOCUMENT CONTROL DATA - R & D

(Security classification of title, body of abstract and indexing annotation must be entered when the overall report is classified)

1. ORIGINATING ACTIVITY *(Corporate author)*

U. S. Naval Ordnance Laboratory
White Oak, Silver Spring, Maryland

2a. REPORT SECURITY CLASSIFICATION

UNCLASSIFIED

2b. GROUP

3. REPORT TITLE

A STUDY OF THE ROLE OF MECHANICAL-STRENGTH PROPERTIES ON THE PHENOMENA OF SPALLATION

4. DESCRIPTIVE NOTES *(Type of report and inclusive dates)*

5. AUTHOR(S) *(First name, middle initial, last name)*

Piacesi, Robert and
Watt, James W.

6. REPORT DATE	7a. TOTAL NO. OF PAGES	7b. NO. OF REFS
4 January 1966	26	13

8a. CONTRACT OR GRANT NO.	9a. ORIGINATOR'S REPORT NUMBER(S)
b. PROJECT NO.	NOLTR 66-42
c.	9b. OTHER REPORT NO(S) *(Any other numbers that may be assigned this report)*
d.	Ballistics Research Report 157

10. DISTRIBUTION STATEMENT

Distribution of this document is unlimited.

11. SUPPLEMENTARY NOTES	12. SPONSORING MILITARY ACTIVITY

13. ABSTRACT

An experimental investigation was made to determine the role of mechanical-strength properties on the spallation phenomena due to hypervelocity impact. The size of the impacting particle and the thickness of the target were held constant, while the impacting velocity and the yield strength of the target were varied. The spall location, the magnitude of the shock wave arriving at the target's rear surface, and the amount of bulging of the spall piece were measured. The bulging could be predicted with theory to good agreement.

14 KEY WORDS	LINK A		LINK B		LINK C	
	ROLE	WT	ROLE	WT	ROLE	WT
Hypervelocity impact Spallation Shock wave propagation Impact damage						